CHEMSUSCHEM

DOI: 10.1002/cssc.200900196

Self-Assembly of Thiophene- and Furan-Appended Methanofullerenes with Poly(3-Hexylthiophene) in Organic Solar Cells

Pavel A. Troshin,*[a] Ekaterina A. Khakina,[a] Martin Egginger,[b] Andrey E. Goryachev,[a] Sergey I. Troyanov,[c] Anita Fuchsbauer,[b] Alexander S. Peregudov,[d] Rimma N. Lyubovskaya,[a] Vladimir F. Razumov,[a] and N. Serdar Sariciftci[b]

Novel fullerene derivatives bearing thiophene and furan residues were synthesized and studied as electron acceptor materials in bulk heterojunction organic solar cells, together with poly(3-hexylthiophene) (P3HT) as the donor polymer. Some compounds showed large nanomorphological inhomogenities in blends with P3HT; in particular, clusters with dimensions in the range of 100–1000 nm were formed. However, some blends that showed such large clusters yielded at the same time high power conversion efficiencies in photovoltaic devices, approaching 3.7%. This is in sharp contrast with previously studied systems, in which a substantial phase separation always resulted in a poor photovoltaic performance. We assume that the attachment of thienyl or furyl groups to the fullerene cage results in a certain ordering of the designed fullerene derivatives **I**–**IX** with P3HT in photoactive blends. Both the fullerene derivative and P3HT might assemble via π–π stacking of the thiophene units to form the nanostructures observed in the films by optical and atomic force microscopy. The presence of ordered donor and acceptor counterparts in these nanostructures results in superior photovoltaic device operation.

Introduction

Intensive research efforts in the field of organic photovoltaics during the last 15 years has resulted in a gradual improvement of the efficiencies of organic solar cells, up to the level of 4–6% achieved during the period 2005–2008.[1–7] Therefore, organic solar cells are nowadays taken into account seriously as one of several promising approaches for harvesting sunlight. The most important breakthroughs in the history of organic photovoltaics are related to the design and application of novel photoactive materials, in particular, conjugated polymers.[6] Thus, poly(*p*-phenylenevinylenes) were among the first electron-donating polymers successfully used in photovoltaic devices, followed by poly(3-alkylthiophenes), particularly, by regioregular poly(3-hexylthiophene) (P3HT), which in turn is now being replaced by a new generation of low-band-gap donor polymers.[2,3,8] The electron acceptor counterpart of the conjugated polymers is usually the pristine fullerene C_{60} or one of its highly soluble derivatives. The fullerene derivative phenyl-C_{61}-butyric acid methyl ester ([60]PCBM), first synthesized by Hummelen and co-workers,[9] and the analogous C_{70} derivative [70]PCBM[10] are nowadays commonly used in organic solar cells.[11]

Researchers have already tested fullerene derivatives with attached chromophore units such as perylene,[12] phthalocyanine,[13] and cyanine dye frameworks,[14] some cross-linkable fullerene derivatives,[15] dimers and oligomers,[16] pyrrazollinofullerenes bearing electron-deficient groups,[17] fullerene compounds with appended malonic acid ester residues,[18] and a number of other compounds that bear bulky solubilizing groups.[19–20] However, there are few examples of fullerene derivatives in organic solar cells that in combination with P3HT showed power conversion efficiencies exceeding 2%, such as di(4′-dodecyloxyphenyl)-C_{61} methanofullerene,[21] the butyl ester of phenyl-C_{61}-butyric acid (PCBB),[22] series of PCBM derivatives with 2-ethylhexyloxy side chains,[23] a bis-addition product bearing two PCBM-type addends on the fullerene cage,[24] dihydronaphthyl-bridged ester derivatives,[25] and a thiophene-based modification of PCBM called ThCBM.[26] The three latter

[a] *Dr. P. A. Troshin, E. A. Khakina, A. E. Goryachev, Prof. R. N. Lyubovskaya, Prof. V. F. Razumov*
Institute for Problems of Chemical Physics
Russian Academy of Sciences
Semenov Prospect 1, Chernogolovka, Moscow Region, 142432 (Russia)
Fax: (+7)-496-515-54-20
E-mail: troshin@cat.icp.ac.ru

[b] *Dr. M. Egginger, A. Fuchsbauer, Prof. N. S. Sariciftci*
Linz Institute for Organic Solar Cells (LIOS)
Johannes Kepler University Linz
Altenbergerstrasse 69, 4040 Linz (Austria)

[c] *Prof. S. I. Troyanov*
Department of Chemistry
Moscow State University
Leninskie Gory, Moscow, 119991 (Russia)

[d] *Prof. A. S. Peregudov*
A. N. Nesmeyanov Institute of Organoelement Compounds
Vavylova St. 28, B-334, Moscow, 119991 (Russia)

Supporting Information for this article is available on the WWW under http://dx.doi.org/10.1002/cssc.200900196.

compounds were the most efficient and yielded power conversion efficiencies of $>3.0\,\%$ in solar cells together with P3HT.

Recently we have reported an investigation of 27 methanofullerenes used as electron-acceptor materials in bulk heterojunction organic solar cells with P3HT.[27] An important correlation was revealed between the solubility of the fullerene derivatives, the nanomorphology of their blends with P3HT, and the performance of solar cells comprising these blends in their active layers. However, a few compounds did not fit so well to the trends revealed for the vast majority of the fullerene derivatives. We assumed that the most probable reason for the observed deviations was the ability of some compounds to self-assemble with the donor polymer P3HT. Herein, we address this issue in greater detail. For this purpose we prepared methanofullerenes **I**–**IX** (Figure 1) and investigated them as electron-acceptor materials in P3HT-based organic solar cells. The peculiarity of these compounds lies in the presence of 2-furyl and 2-thienyl substituents in their molecular frameworks. These substituents might promote self-assembly of the fullerene derivatives with thiophene units of the P3HT backbone via π–π stacking interactions.

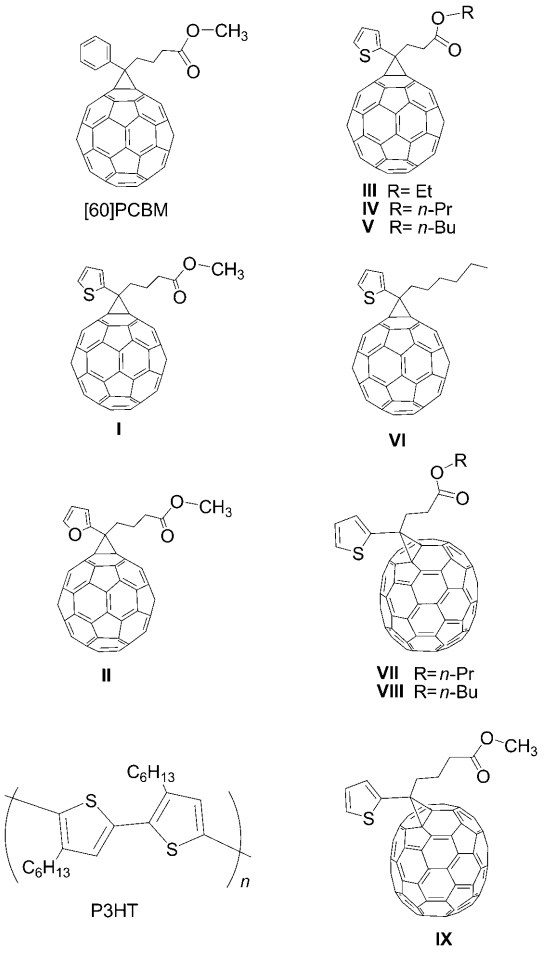

Figure 1. Molecular structures of the synthesized fullerene-based materials and P3HT used in organic solar cells.

Results and Discussion

Synthesis and properties of the fullerene derivatives

Compounds **I**–**IX** were synthesized according to the routes outlined in Schemes 1–3. First, commercially available 4-methoxycarbonylbutyric acid was converted to chloroanhydride **1**. The acylation of thiophene by **1** proceeded smoothly in dried chlorobenzene as solvent with tin tetrachloride as catalyst. An attempted acylation of furan with cyclic anhydride of glutaric acid with magnesium perchlorate as catalyst or with **1** failed due to the formation of a mixture of resinous products. Alternatively, anhydride **4** was prepared from 4-methoxycarbonylbutyric acid and chloroanhydride **1** and used for the acylation of furan catalyzed by boron trifluoride, which yielded the desired product **5**. The prepared 2-thienyl- and 2-furylsubstituted ketones **2** and **5** were converted to the corresponding tosylhydrazones **3** and **6**. The treatment of tosylhydrazones with C_{60} under conditions established by Hummelen and co-workers for PCBM[9] yielded the title compounds **I**, **II**, and **IX**.

Three different 3-alkoxycarbonylpropionic acids **7a**–**c** were easily obtained from succinic anhydride and alcohols and used as key precursors for the preparation of compounds **III**–**V** and **VII**–**VIII**. The conversion of acids **7a**–**c** to chloroanhydrides **8a**–**c**, the acylation of thiophene, the transformation of the resulting ketones **9a**–**c** to tosylhydrazones **10a**–**c** and, finally, their reactions with fullerenes C_{60} and C_{70} yielding **III**–**V** and **VII**–**VIII** closely resemble the sequence of stages used for the preparation of **I**. Similarly, we synthesized compound **VI** starting from heptanoyl chloride and thiophene.

The compositions and molecular structures of the prepared fullerene derivatives were confirmed by ^{1}H and ^{13}C NMR. Figure 2 shows representative spectra obtained for compound **IV** with the assignment of some signals. The high purity (98 %+) of the prepared compounds was confirmed by NMR spectroscopy, chemical analysis data, and, in some cases, by HPLC (see Supporting Information). We note that derivatives of [70]fullerenes **VII**–**IX** were obtained as mixtures of three isomers formed via additions across 1,2- and 5,6-double bonds in the C_{70} cage. As soon as the cyclopropane ring attached to the fullerene cage bears two different substituents (a 2-thienyl group and a residue of propionic or butyric acid ester), the 5,6-addition pattern gives two stereoisomers. The content of the major 1,2-isomer estimated by NMR spectroscopy (see Supporting Information) was 85–91 %, which is much higher than the content of the two other isomeric products (9–15 % total). Therefore, we assume that the structures of the main 1,2-isomers drawn for compounds **VII**–**IX** accurately represent their compositions. Similar results were reported previously for [70]PCBM that was also obtained as a nonseparable mixture of isomers, and successfully applied as a photoactive material in organic solar cells.[10]

The fullerene derivatives exhibited notably different solubilities in organic solvents, in particular in chlorobenzene, which is the typical solvent used for active layer deposition in the laboratory preparation of solution-processed organic solar cells. Therefore, we measured the solubility of **I**–**IX** in chloro-

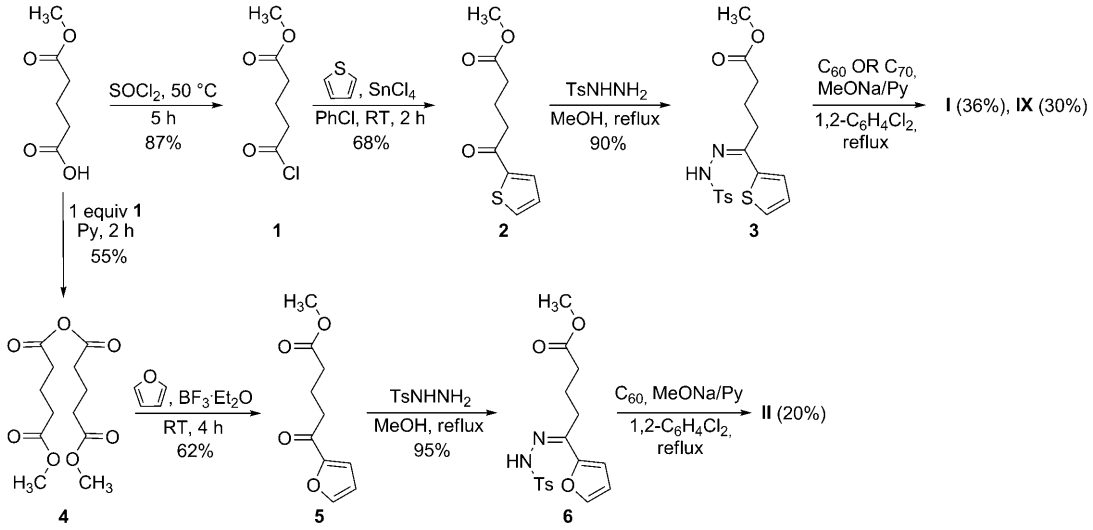

Scheme 1. Synthesis of fullerene derivatives **I**, **II**, and **IX**.

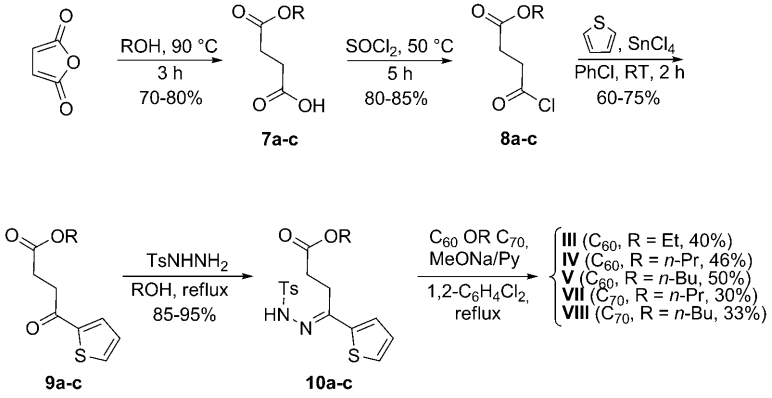

Scheme 2. Synthesis of fullerene derivatives **III**–**V**, **VII**, and **VIII**.

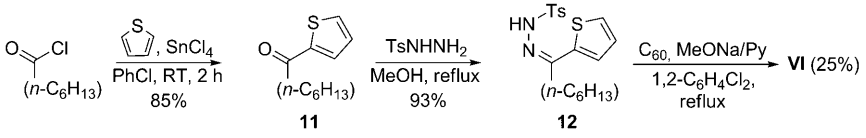

Scheme 3. Synthesis of fullerene derivative **VI**.

benzene. The obtained values are listed in Table 1. Compound **III** was the least soluble: its solubility hardly reached 1 mg mL^{-1}, which is 5–10 times lower than the solubility of the nonfunctionalized fullerene C_{60}. In contrast, the thiophene-containing compounds **I**, **IV**, **V**, and **IX** showed considerably higher solubility values of 30–70 mg mL^{-1} while the solubility of C_{70} derivatives **VII**–**VIII** exceeded 100 mg mL^{-1}. The furyl-substituted compound **II** had a solubility of 58 mg mL^{-1}, which is very close to the solubility of [60]PCBM (50 mg mL^{-1}).

To obtain single crystals of our new materials we slowly concentrated their solutions in organic solvents by evaporating the solvent. This procedure sometimes yielded single crystals of compounds **I** and **III**–**IV** that presumably comprise both the fullerene derivatives and solvent molecules arranged together in the crystal lattice. Such adducts formed by solvation are generally called solvates. Recently we investigated a large family of similarly substituted methanofullerenes and showed that the performance of these materials in organic solar cells depends on their solubility in the solvents used for the film deposition.[27] Interestingly, the solubility of some very similar compounds differed significantly in some cases. In general, there was no clear correlation found between the solubility of the fullerene derivatives and their molecular structure. To explain the observed nonpredictable change in solubility, we suggested that the fullerene derivatives form solvates with the solvent molecules. The stability and other properties of such solvates might be very different even for structurally similar compounds.

This assumption about the formation of solvates is now proven by X-ray single-crystal structure determination for the 1:1 solvate of compound **IV** with chlorobenzene. X-ray diffraction confirmed the structure of compound **IV** and revealed that it indeed possesses a cyclopropane unit attached across the 6–6 ring junction onto the fullerene cage with two substituents: 2-thienyl and 2-(*n*-propyloxycarbonyl)ethyl. This molecular structure is also supported by the ^{1}H and ^{13}C NMR spectra (Figure 2). The respective orientation of the fullerene derivative and the solvent molecules (chlorobenze) and their packing in the crystal of the adduct **IV**·C_6H_5Cl are shown in Figure 3. It is interesting to note that any short π–π interactions between the thiophene rings of two neighboring molecules of **IV** as well as between the thiophene groups of one molecule and the fullerene cage of an-

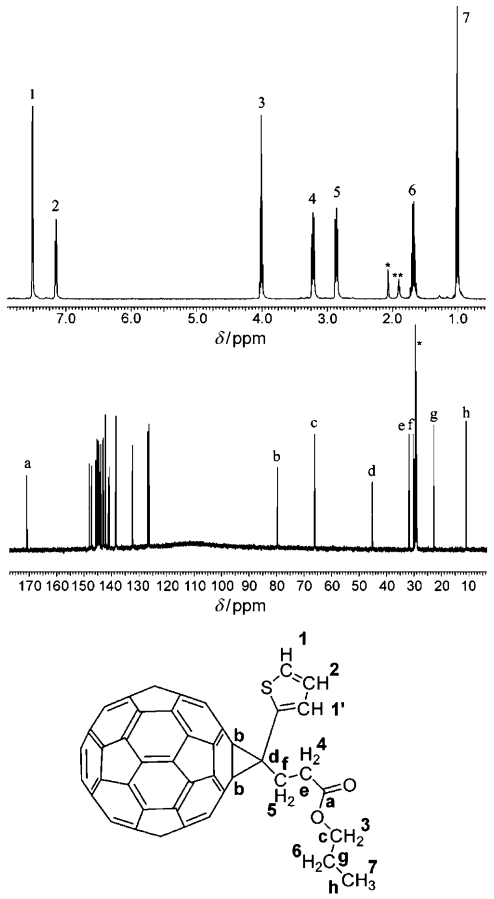

Figure 2. a) ^{1}H NMR and b) ^{13}C NMR spectra of compound **IV**, with c) the assignment of some signals.

Table 1. The performances of compounds **I–IX** as electron acceptor materials in P3HT-based solar cells.[a]

Compound	Solubility[b] [mg mL^{-1}]	I_{sc} [mA cm^{-2}]	V_{oc} [mV]	*FF* [%]	η [%]
[60]PCBM	50 (PhCl)	10.6	640	55	3.7
I	36 (PhCl)	10.8	590	57	3.7
II	58 (PhCl)	7.9	600	33	1.2
III[c]	23 (CS_2)	8.4	600	50	2.5
IV	45 (PhCl)	10.2	600	54	3.4
V	70 (PhCl)	9	600	53	2.9
VI	25 (PhCl)	8	580	45	2.1
VII	130 (PhCl)	4.6	590	41	1.1
VIII	124 (PhCl)	4.4	590	43	1.1
IX	55 (PhCl)	10.1	600	63	3.8

[a] All devices were annealed at 155–160 °C for 5 min after Al cathode deposition. [b] Solubility in solvent used for film-casting; PhCl: chlorobenzene, CS_2: carbon disulfide. [c] Solubility of **III** in chlorobenzene: <1 mg mL^{-1}.

other are missing in this structure. In contrast, such intermolecular contacts are quite typical for many other known thiophene-containing systems, in particular, for poly(3-hexylthiophene) and some thiophene-based oligomers.[28]

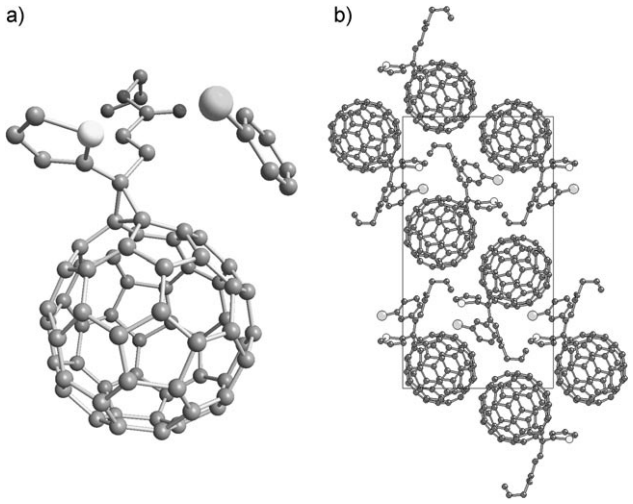

Figure 3. The relative orientation of fullerene derivative **IV** and chlorobenzene molecules in a) the solvate **IV**·C_6H_5Cl and b) their packing in the crystal lattice.

Thin films of fullerene-derivative/polymer blends

P3HT is the benchmark for electron donor polymers in organic solar cells. PCBM is routinely blended with a comparable weight fraction of P3HT to yield composites with a variable degree of phase separation between the components. Evidence that the nanomorphology of PCBM/P3HT blends has a crucial influence on their performance in organic solar cells has been documented in numerous studies.[5] The optimal degree of phase separation in these blends is believed to be that at which distinct P3HT-rich and PCBM-rich clusters approach a size of approximately 10–20 nm. This dimension is comparable to typical exciton diffusion lengths in organic semiconductors.[6,29] The controlled optimization of the blend morphology is typically achieved by thermal annealing of as-cast PCBM/P3HT blend films at temperatures of 120–150 °C for 5–30 min.

Here we explored the possibility to induce some component ordering in the fullerene/P3HT blends by using intermolecular assembly effects. The aggregation of PCBM as well as other fullerene derivatives is governed by intermolecular van der Waals attractions of the molecules, sometimes even by an additional stacking of their π-systems. We assume that the designed fullerene derivatives **I–IX** bearing thiophene or furan moieties appended to the fullerene cage will be capable of π–π stacking with thiophene units in the polymer backbone. Such intermolecular interactions between the components in the blend might enforce co-dissolving of the fullerene derivatives and the polymer to some extent, and the stabilization of the resulting solid solutions. In other words, the attachment of thienyl or furyl groups to the fullerene cage might improve the intermiscibility of such derivatives with the thiophene polymer. Note that in particular compound **VI** bears a group that closely resembles the repeat unit of P3HT.

In order to reveal self-assembly effects we investigated the nanomorphology of fullerene/polymer composite thin films deposited onto poly(3,4-ethylenedioxythiophene):poly(styrenesulfonate) films on indium tin oxide substrates (ITO/PEDOT:PSS)

under the same conditions as for the fabrication of photovoltaic cells. In some cases finalized devices were used to obtain optical microscopy and atomic force microscopy (AFM) images from the film area selected between the electrodes.

Microscopy studies revealed that the blends of fullerene derivatives **I**, **II**, and **VI** with P3HT exhibited large inhomogenities at the film surface (Figure 4). Similar structures appearing in PCBM–polymer blends are usually interpreted as aggregates of pure PCBM that have segregated from the polymer, as was shown for PCBM/MDMO:PPV composites.[30] Therefore, the observed surface inhomogenities suggest a relatively high degree of phase separation in the blends of **I**, **II**, and **VI** with P3HT. This film topology is remarkably stable with respect to thermal annealing at 165 °C for 10–30 min. The AFM images in Figure 4 show that annealing of the films at 165 °C for 10 min does not dramatically change the surface roughness.

A different situation was observed for films of the same of **I**/P3HT and **II**/P3HT blends cast directly onto glass slides (without ITO and PEDOT:PSS underlayers). Thermal annealing of these films for 5–10 min resulted in the appearance of aggregate structures visible even with the naked eye. Optical microscopy images of **I**/P3HT and **II**/P3HT blend films before and after annealing are shown in Figure 5. The seed-like structures, 10–20 μm long and 0.3–0.5 μm thick, can be clearly seen on the images of the annealed films. An unusual film topology was revealed by AFM for **I**/P3HT blends in the areas between the large seed-like clusters. Considering the image shown in Figure 5 d, one can assume that some nanofibers 100–200 nm thick and few micrometers long appear in the **I**/P3HT blends. These results suggest that heating induces strong cluster formation and, most likely, a phase separation in the blend films coated directly on glass slides. The origin of such substrate-dependent phase separation behavior is not clear at present.

The next important issue to be addressed is the composition of the aggregates formed in the blends of fullerene derivatives **I**, **II**, and **VI** with P3HT. These might be clusters of pure fullerene derivatives (**I**, **II**, or **VIII**) that segregated from the polymer like in the case of PCBM/MDMO:PPV system.[30] Considering that the exciton diffusion lengths in organic semiconductors usually do not exceed 20 nm[31] while the structures observed in the thermally annealed blends cast on PEDOT:PSS are much larger and approach 1000 nm in size. Therefore, most of the

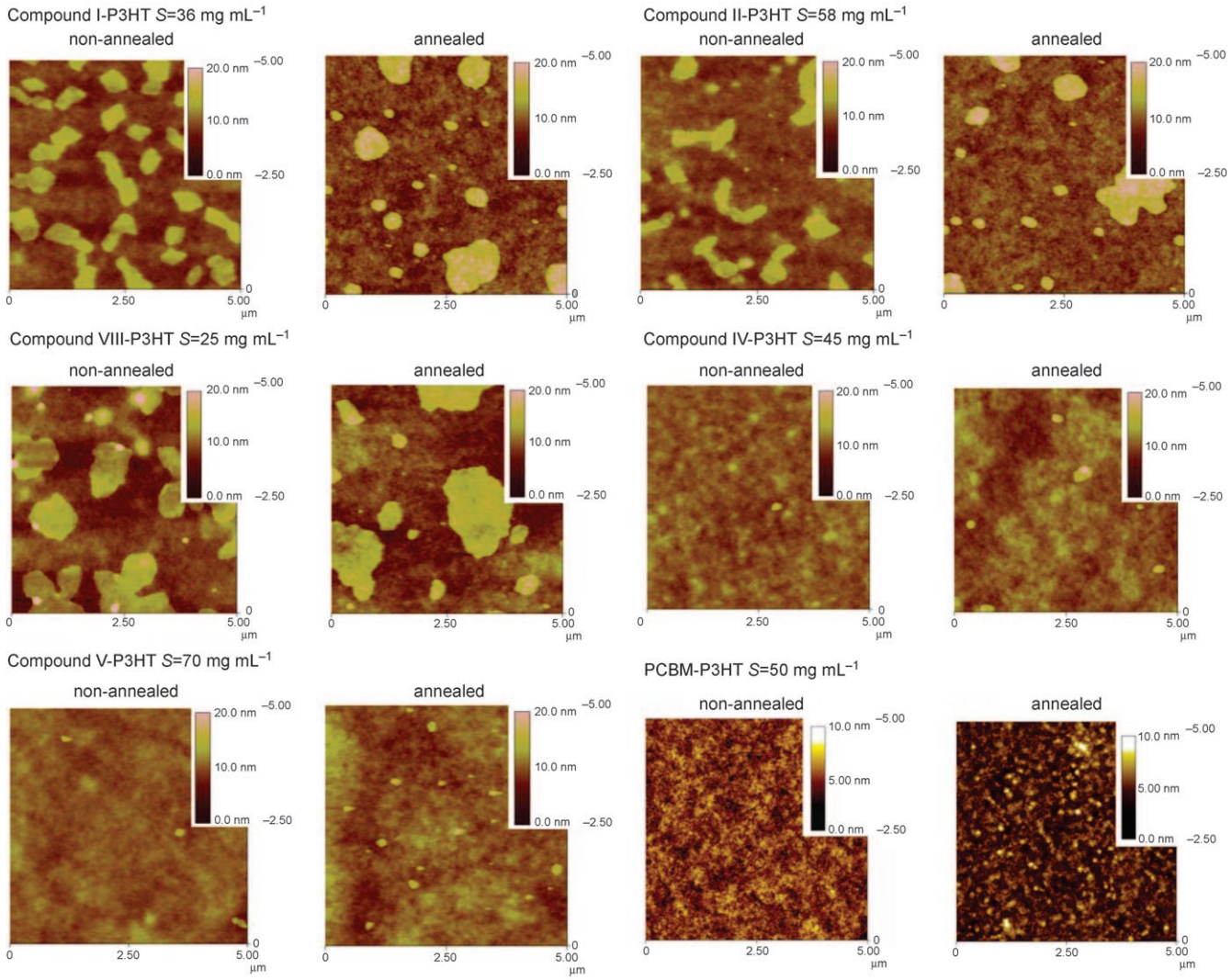

Figure 4. AFM images of fullerene-derivative/P3HT blend films with a 2:3 component ratio (w/w) spin-coated onto PEDOT:PSS films.

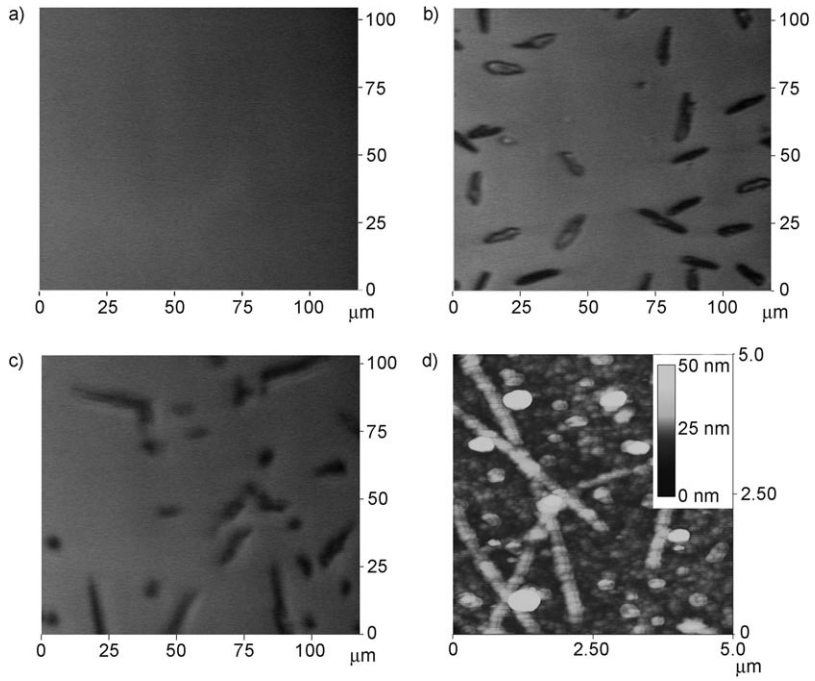

Figure 5. Optical microscopy images of non-annealed a) **I**/P3HT blend; an image of the non-annealed **II**/P3HT blend was identically featureless. Optical images of the annealed blends of P3HT with b) compound **I** or c) compound **II** spin-coated onto glass substrates. d) AFM image of the annealed **I**/P3HT blend film on glass measured in a "smooth" area between large clusters.

excitons photogenerated inside these large fullerene clusters should recombine before they can approach an interface with the polymer where charge separation can happen. This should result in significant recombination losses reflected in decreased photocurrents in the photovoltaic devices. However, the solar cells comprising compounds **I**, **II**, or **VI** in a bulk heterojunction with P3HT showed photocurrent densities of around 10 mA cm^{-2} (Table 1), which are similar to optimized PCBM/P3HT cells where no large scale segregation of the components was observed. Particularly, the devices based on **I**/P3HT blends yielded even higher currents than the reference PCBM/P3HT devices. The AFM image shown in Figure 5 for the annealed **I**/P3HT blend was obtained directly from the photovoltaic device that yielded current densities as high as 10 mA cm^{-2} together with an appreciable fill factor and a good open circuit voltage, resulting altogether in a power conversion efficiency of 3.7% (Table 1). This shows that the observed large nanostructures in the films of **I**/P3HT participate efficiently in the photocurrent generation and do not disturb the charge-carrier transport in the films (reflected by high fill factors). Such observations suggest that the aggregates observed in the blends of **I**, **II**, and **VI** with P3HT do not consist of pure fullerene derivatives but most probably comprise both the fullerene derivative and the polymer. This enables the photogeneration of charges inside the clusters and their subsequent transport to the respective electrodes.

To prove this suggestion we performed a comparative study of **I**/P3HT and PCBM/P3HT blend films cast directly onto glass substrates. The investigated films were non-annealed (batch 1), annealed at 155 °C for 5 min (batch 2), or at 160 °C for 15 min (batch 3). Optical microscopy revealed no visible phase separation in the films from batch 1 (Figure 6c). However, large clusters were observed in **I**/P3HT blends in batch 2. On the contrary, no aggregates were detected in the PCBM/P3HT composite films in the same batch. Microscopy inspection of the films from batch 3 showed that **I**/P3HT blends have the same morphology as respective samples from batch 2. However, some small clusters were detected in the films of PCBM/P3HT blends from the batch 3 that distinguishes them from the respective samples in batch 2. This observation suggests that annealing of the PCBM/P3HT blends at 160 °C for 15 min induces some cluster formation.

It is useful to follow changes in the absorption spectra of the PCBM/P3HT and **I**/P3HT blends upon thermal annealing. Annealing of both systems resulted in the appearance of an intensive band at ca. 602 nm (see absorption spectra in the Supporting Information, Figs. S21–S22). This band is most pronounced in the spectrum of annealed **I**/P3HT blends and pristine P3HT, and corresponds to the well-organized crystalline polymer domains.[32] At the same time, the films of **I**/P3HT blend absorb more intensely at 530–670 nm in comparison with the respective PCBM/P3HT blend films. These observations suggest that the P3HT-rich phase is more ordered in the blends with compound **I** rather than in the blends with PCBM.

It might be assumed that thermal annealing results in a segregation of the fullerene component from the polymer and, finally, a segregated fullerene phase forms the large aggregates observed by optical microscopy. The segregation of the components in the fullerene-polymer blends can be monitored by measuring the photoluminescence (PL) spectra for the films cast on glass.[33] It is known that the fullerene derivatives quench the polymer PL very efficiently via fast photoinduced electron transfer from the excited states of the polymer.[34] The rate of such an electron transfer process is typically three orders of magnitude higher than the PL rate. Therefore, blends with good intermixing between the components show very weak PL because of efficient quenching. However, segregation between the components makes quenching less efficient and as a consequence PL becomes more pronounced.

In the case of our systems, non-annealed blends PCBM/P3HT and **I**/P3HT demonstrated a 25- and 15-fold stronger quenching with respect to the PL intensity measured for pristine P3HT (Figure 6). Surprisingly, annealing of the blends under mild conditions (155 °C, 5 min) leads to even weaker PL for both

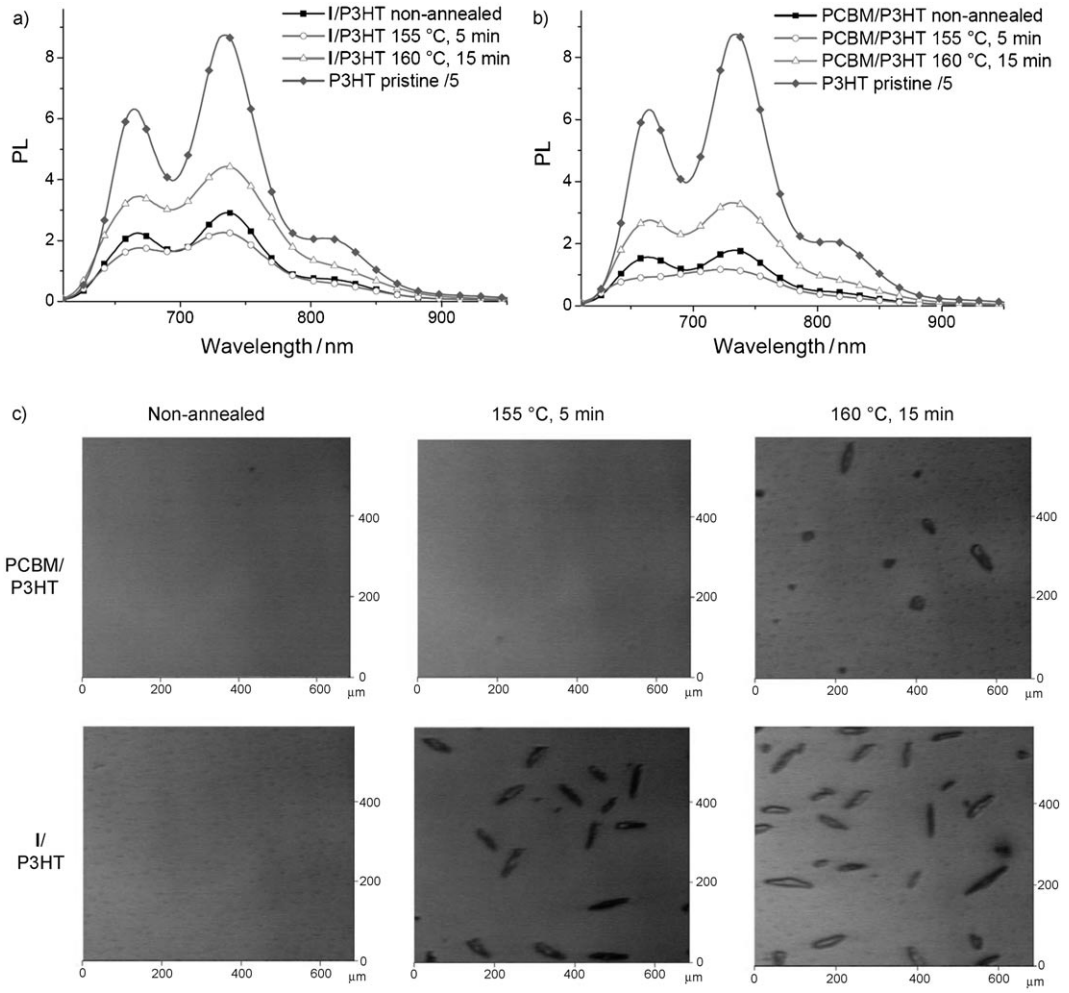

Figure 6. Photoluminescence spectra of pristine P3HT (divided by 5) and blends of a) **I**/P3HT and b) PCBM/P3HT non-annealed and annealed at different temperatures. c) Optical microscopy images of the investigated blends, shown for comparison.

systems. At the same time, longer annealing of the blends at 160 °C for 15 min enhances PL. Such an increase of the PL intensity appears to be a consequence of the thermally induced segregation of the components in the blends. Obviously, this segregation should be very similar for **I**/P3HT and PCBM/P3HT blends, because they show very similar PL properties. However, as stated above, the change of the film topologies upon annealing is sharply different for **I**/P3HT and PCBM/P3HT blends.

It is possible that the film topology does not reflect the real component segregation in the blends. Particularly surprising is that the reduction of the PL intensity for **I**/P3HT blends after annealing at 155 °C is accompanied by the appearance of the large aggregate structures (Figure 6). On the contrary, a dramatic enhancement of the PL is expected for systems in which two components are segregated so strongly from each other, yielding large clusters. Therefore, the observed cluster formation cannot be related to the segregation of the fullerene component from the polymer in **I**/P3HT blends (nor, presumably, in similar **II**/P3HT and **VI**/P3HT blends). This means that the observed clusters indeed comprise both fullerene and polymer components.

This situation resembles binary solid systems with limited solubilities of the components in each other. One can find two coexisting phases in such systems and each of these phases is represented by a solid solution of one component in another. Similarly, the investigated blends seem to comprise coexisting solutions of the fullerene derivative in P3HT and P3HT solution in the fullerene phase.

The synthesized fullerene derivatives **I**–**VIII** were tested as electron-acceptor materials in bulk heterojunction organic solar cells using P3HT as electron donor. The device architecture, the current-voltage (*I*–*V*) curves for some representative devices, and the respective IPCE spectra are shown in Figure 7. The obtained solar cell output parameters are listed in Table 1.

No clear correlation was observed between the performance of the materials in devices and the surface topology of their blends with P3HT, revealed by AFM. On the one hand, blends with very different surface topologies can give very similar output characteristics in devices. For example, the **I**/P3HT blend showed large surface irregularities suggesting a high degree of phase separation, while the films of **IV**/P3HT or **IX**/P3HT were very smooth suggesting their high phase homogeneity. Despite such sharply different film topologies, all of these three blends yield comparable power conversion efficiencies of 3.4–3.8 % in solar cells.

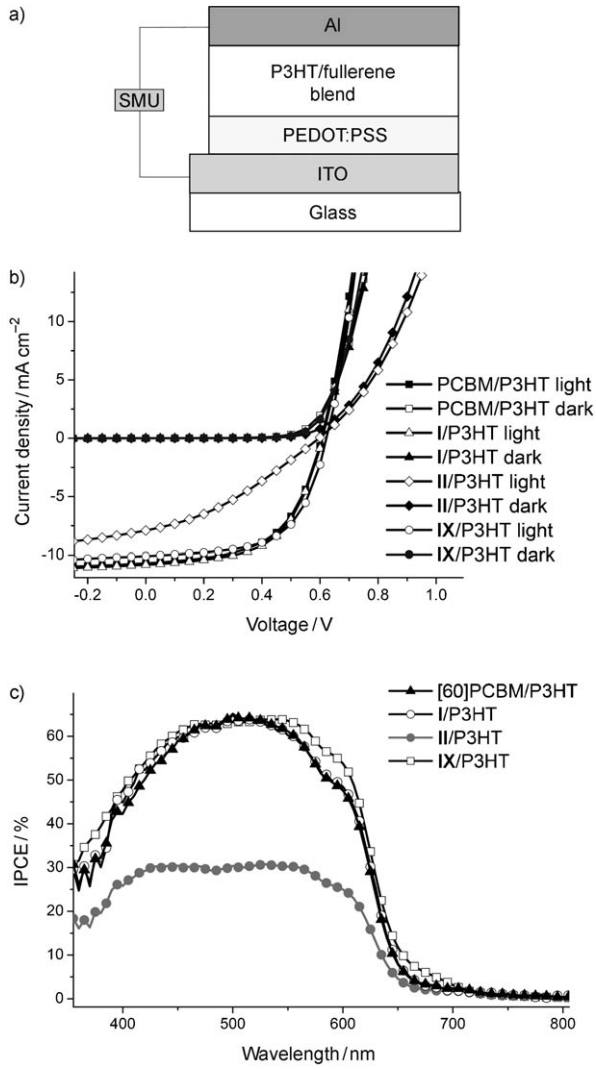

Figure 7. a) Schematic layout of the solar cells, and representative b) *I–V* curves and c) IPCE spectra.

On the other hand, blends with similar surface topologies provided different results in the devices. For example, the blends of fullerene derivatives **I**, **II**, and **VI** with P3HT showed similar large surface inhomogeneities but yielded quite different power conversion efficiencies of ca. 3.7%, ca. 1.2%, and ca. 2.1%, respectively. These representative values with relatively small deviations of $\pm$0.1–0.2% were reproducibly obtained for series of 40–50 devices fabricated with each investigated fullerene derivative.

At the same time, blends of P3HT with compounds **IV**–**V** and **VII**–**IX** or with PCBM gave very smooth films without any notable irregularities. In spite of the film surface similarity, these blends provided power conversion efficiencies in devices ranging from 1.1 to 3.8%, depending on the fullerene compound.

In summary, the surface topology of the fullerene/P3HT films, derived from AFM measurements, does not allow to draw conclusions about the performance of the given material combinations in the solar cells studied here. This is an unexpected observation because in former studies the performance of solar cells was shown to correlate well with the degree of phase separation of the materials in the active layer.[33,35] We assume that the proposed self-assembly of the fullerene derivatives with pendant thiophene units and the thiophene polymer backbone changes these correlations.

We have recently shown that the efficiency of bulk heterojunction photovoltaic devices depends strongly on the relative solubility of the donor and acceptor materials in the solvent used for the blend deposition. In particular, the fullerene derivatives combined with P3HT should have a solubility of 30–50 mg mL^{-1} to achieve the highest performance of such blends in photovoltaic devices. Indeed, compounds **I**, **IV**, and PCBM yielded the best power conversion efficiencies in our experiments because their solubility in chlorobenzene fits within this 30–50 mg mL^{-1} region. A notable exception is compound **II**, which gives low device performance in spite of a good solubility (58 mg mL^{-1}). Low fill factors measured for the photovoltaic cells comprising compound **II** might be explained by unsatisfactory electron transport properties of this material arising from the presence of the furyl unit in its molecular framework. This aspect needs to be clarified in a subsequent study.

The fullerene derivatives **III** and **VI** (as well as **VII** and **VIII**) possess similar solubilities, resulting in similar device performances. Table 1 also shows that compounds with solubilities lower than 30 mg mL^{-1} or higher than 50 mg mL^{-1} give reduced performances in the devices in comparison with the compounds **I**, **IV**, and PCBM. Thus, the solubility of the materials should be counted as an important parameter in device optimization. Compound **III** was almost insoluble in chlorobenzene, therefore it was blended with P3HT using carbon disulfide as a solvent where solubility of **III** was estimated as 23 mg mL^{-1}.

We note that compound **I** was prepared before and named "[60]ThCBM".[26] The authors reported a power conversion efficiency of 3% for their [60]ThCBM/P3HT solar cells, which is lower than typical values reported for a PCBM/P3HT system. Here we processed compound **I** and PCBM under fully identical conditions and obtained almost identical output parameters and solar simulator power conversion efficiencies of 3.7%. At the same time, solar cells based on **I**/P3HT blends showed superior stability. The output parameters of the cells comprising **I** decreased by only 2–4% after thermal annealing at 160 °C for 30 min. On the contrary, device performance drops of ca. 25–35% were observed for the reference PCBM/P3HT composites annealed under the same conditions. Therefore, [60]ThCBM should be considered as a promising material for organic photovoltaics that might improve the long-term stability of the devices.

Compound **IX** ([70]ThCBM), seems to be an even-more-promising material than compound **I**. High power conversion efficiencies of ca. 3.8% were reproducibly obtained for devices based on blends of **IX** with P3HT processed even under non-optimized conditions.

Conclusions

A range of 2-thienyl- and 2-furyl-substituted methanofullerenes was synthesized and characterized, and the materials were in-

vestigated as electron acceptors in organic bulk heterojunction solar cells. Depending on the fullerene derivative used as acceptor material, power conversion efficiencies of 1.1–3.8% were obtained in solar cells. The intermolecular interactions between the thiophene- or furan-appended fullerene derivatives and the P3HT hold them together in solid solutions, which results in an improved stability of the composites upon sintering. Such an intermolecular stabilization of the nanomorphology of fullerene-polymer blends might be considered as a promising way to improve the lifetime of organic photovoltaics in the future.

Experimental Section

Synthesis

Monomethyl esters **7a–c** and chloroanhydrides **1** and **8a–c** were prepared according to a method described in Ref. [36]. The acylations of thiophene with **1**, **8a–c**, and heptanoyl chloride were carried out adopting a procedure reported for the preparation of 2-acetoxythiophene in Ref. [37]. Anhydride **4** and ketone **5** were synthesized according to known procedures [38,39].

Compound **1**: ^{1}H NMR ($CDCl_3$, 600 MHz): $\delta = 2.03$ (m, 2H), 2.40 (t, 2H), 3.61 (t, 2H), 3.69 ppm (s, 3H).

Compound **2**: ^{1}H NMR ($CDCl_3$, 600 MHz): $\delta = 2.07$ (m, 2H), 2.45 (t, 2H), 2.99 (t, 2H), 3.68 (s, 3H), 7.15 (t, 1H), 7.63 (d, 1H), 7.74 ppm (d, 1H).

Compound **4**: ^{1}H NMR ($CDCl_3$, 600 MHz): $\delta = 2.43$ (t, 4H), 2.55 (t, 4H), 2.99 (m, 4H), 3.69 ppm (s, 6H).

Compound **5**: ^{1}H NMR ($CDCl_3$, 600 MHz): $\delta = 2.07$ (m, 2H), 2.45 (t, 2H), 2.92 (t, 2H), 3.70 (s, 3H), 7.15 (t, 1H), 7.22 (d, 1H), 7.65 ppm (t, 1H).

Compound **8c**: ^{1}H NMR ($CDCl_3$, 600 MHz): $\delta = 0.90$ m, (t, 3H), 1.35 (m, 2H), 1.58 (m, 2H), 2.64 (t, 2H), 3.18 (t, 2H), 4.07 ppm (t, 2H).

Compound **9a**: ^{1}H NMR ($CDCl_3$, 600 MHz): $\delta = 1.08$ (t, 3H), 2.57 (t, 2H), 3.09 (t, 2H), 3.96 (q, 2H), 6.96 (t, 1H), 7.50 (d, 1H), 7.61 ppm (d, 1H).

Compound **9b**: ^{1}H NMR ($CDCl_3$, 600 MHz): $\delta = 0.81$ (t, 3H), 1.51 (m, 2H), 2.63 (t, 2H), 3.13 (t, 2H), 3.92 (t, 2H), 7.00 (t, 1H), 7.53 (d, 1H), 7.64 ppm (d, 1H).

Compound **9c**: ^{1}H NMR ($CDCl_3$, 600 MHz): $\delta = 0.88$ (t, 3H), 1.34 (m, 2H), 1.57 (m, 2H), 2.72 (t, 2H), 3.21 (t, 2H), 4.06 (t, 2H), 7.09 (t, 1H), 7.61 (d, 1H), 7.73 ppm (d, 1H).

Compound **11**: ^{1}H NMR ($CDCl_3$, 600 MHz): $\delta = 0.87$ (t, 3H), 1.30 (m, 6H), 1.72 (m, 2H), 2.86 (t, 2H), 7.09 (t, 1H), 7.59 (d, 1H), 7.68 ppm (d, 1H).

Tosylhydrazones **3**, **6**, **10a–c**, and **12**: A mixture of the ketone (**2**, **5**, **9a–c**, or **11**; 20 mmol), tosylhydrazide (22 mmol), and methanol (25 mL) was heated at reflux for 1 h. Afterwards it was cooled to room temperature and left overnight in a refrigerator at 4–5 °C to stimulate the crystallization of the product. The crystalline precipitate was isolated by filtration, washed with a small amount of methanol (2–5 mL), and dried in air. A single isomer or a mixture of two stereoisomers of the corresponding tosylhydrazones was formed in total yields of 80–95%.

Compound **3**: ^{1}H NMR ($CDCl_3$, 600 MHz): $\delta = 1.75$ (m, 2H), 2.33 (t, 2H), 2.42 (s, 3H), 2.63 (t, 2H), 3.81 (s, 3H), 6.99 (t, 1H), 7.19 (d, 1H), 7.31 (m, 3H), 7.92 (d, 2H), 9.03 ppm (s, 1H).

Compound **6** (mixture of 2 isomers): ^{1}H NMR ($CDCl_3$, 600 MHz): $\delta =$ 1.72 (m, 1H), 1.89 (m, 2H), 2.27 (t, 2H), 2.33 (t, 1H), 2.42 (s, 1.5H), 2.43 (s, 3H), 2.58 (m, 3H), 3.68 (s, 3H), 3.80 (s, 1.5H), 6.42 (t, 0.5H), 6.53 (t, 1H), 6.71 (d, 0.5H), 6.79 (d, 1H), 7.33 (m, 3H), 7.43 (s, 0.5H), 7.59 (s, 1H), 7.88 (d, 2H), 7.91 (d, 1H), 9.16 (s, 0.5H), 9.42 ppm (s, 1H).

Compound **10a**: ^{1}H NMR ($CDCl_3$, 600 MHz): $\delta = 1.19$ (t, 3H), 2.42 (s, 3H), 2.72 (t, 2H), 2.91 (t, 2H), 4.05 (q, 2H), 6.99 (t, 1H), 7.11 (d, 1H), 7.29 (m, 3H), 7.92 (d, 2H), 9.82 ppm (s, 1H).

Compound **10b**: ^{1}H NMR ($CDCl_3$, 600 MHz): $\delta = 0.92$ (t, 3H), 1.58 (m, 2H), 2.44 (s, 3H), 2.66 (t, 2H), 2.86 (t, 2H), 3.94 (t, 2H), 6.94 (t, 1H), 7.12 (d, 1H), 7.24 (m, 3H), 7.75 (d, 2H), 9.55 ppm (s, 1H).

Compound **10c**: ^{1}H NMR ($CDCl_3$, 600 MHz): $\delta = 0.91$ (t, 3H), 1.31 (m, 2H), 1.51 (m, 2H), 2.42 (s, 3H), 2.70 (t, 2H), 2.90 (t, 2H), 4.00 (t, 2H), 6.99 (t, 1H), 7.12 (d, 1H), 7.29 (m, 3H), 7.94 (d, 2H), 9.83 ppm(s, 1H).

Compound **12**: ^{1}H NMR ($CDCl_3$, 600 MHz): $\delta = 0.87$ (t, 3H), 1.30 (m, 6H), 1.51 (m, 2H), 2.43 (s, 3H), 2.57 (t, 2H), 6.99 (t, 1H), 7.20 (d, 1H), 7.33 (m, 3H), 7.60 (s, 1H), 7.93 ppm (d, 2H).

Methanofullerenes **I–VIII** were prepared from the corresponding fullerenes and tosylhydrazones, according to a method described in Ref [9] for the synthesis of PCBM.

Compound **I** (36%): ^{1}H NMR ($CDCl_3$, 600 MHz): $\delta = 2.36$ (m, 4H), 3.10 (t, 2H), 3.78 (s, 3H), 7.30 (t, 1H), 7.64 (d, 1H), 7.64 ppm (d, 1H). ^{13}C NMR (CS_2-acetone D6, 150 MHz): $\delta = 30.31$, 33.53, 34.19, 46.01, 51.2, 79.94, 126.37, 126.55, 131.96, 138.37, 138.4, 139.14, 140.83, 141.09, 142.18, 142.23, 143.03, 143.1, 143.15, 143.18, 143.89, 144.34, 144.64, 144.72, 144.79, 144.83, 144.87, 145.18, 145.24, 145.28, 145.31, 145.73, 147.5, 148.23, 171.62 ppm. FTIR spectrum (KBr pellet): $\tilde{\nu} = 526$(VS), 554(W), 572(W), 584(W), 668(W), 704(M), 712(M), 742(W), 846(W), 1050(W), 1138(M), 1174(W), 1188(M), 1236(M), 1250(W), 1384(W), 1428(M), 1456(W), 1728(VS), 2330(M), 2360(M), 2848(M), 2918 cm^{-1}(M). UV/Vis: 335, 405, 433, 502 nm. MALDI-TOF MS $m/z = 916$ a.m.u. [M^+].

Compound **II** (20%): ^{1}H NMR ($CDCl_3$, 600 MHz): $\delta = 2.22$ (m, 2H), 2.60 (t, 2H), 2.97 (t, 2H), 3.72 (s, 3H), 6.58 (d, 1H), 6.85 (t, 1H), 7.65 ppm (d, 1H). ^{13}C NMR (CS_2-acetone D6, 150 MHz): $\delta = 30.31$, 31.16, 33.44, 43.97, 78.1, 110.5, 113.14, 138.08, 138.47, 140.85, 141.08, 142.21, 142.24, 142.29, 142.99, 143.05, 143.1, 143.17, 143.86, 143.91, 144.36, 144.63, 144.75, 144.78, 144.81, 144.86, 145.24, 145.29, 145.38, 145.77, 147.28, 148.25, 149.05, 171.71, 192.61 ppm. FTIR spectrum (KBr pellet): $\tilde{\nu} = 526$(VS), 554(M), 574(M), 584(M), 596(W), 684(M), 740(S), 814(M), 880(M), 918(M), 946(M), 988(M), 1010(M), 1062(M), 1072(M), 1156(S), 1176(S), 1186(S), 1210(M), 1248(M), 1366(M), 1428(S), 1732 cm^{-1}(VS). UV/Vis: 335, 405, 433, 502 nm. MALDI-TOF MS $m/z = 900$ amu [M^+].

Compound **III** (40%): ^{1}H NMR (CS_2-acetone D6, 600 MHz): $\delta = 1.24$ (t, 3H), 2.79 (t, 2H) 3.15 (t, 2H), 4.04 (q, 2H), 7.08 (t, 1H), 7.45 ppm (m, 2H). ^{13}C NMR (CS_2-acetone D6, 150 MHz): $\delta = 14.72$, 30.31, 31.85, 45.14, 60.58, 79.77, 125.54, 126.41, 126.85, 128.42, 129.14, 132.37, 137.44, 138.41, 138.43, 138.54, 140.83, 141.1, 142.16, 142.24, 142.26, 143.03, 143.05, 143.11, 143.15, 143.88, 143.89, 144.36, 144.64, 144.66, 144.73, 144.77, 144.88, 145.18, 145.24, 145.28, 145.3, 145.32, 145.74, 147.31, 148.15, 170.78 ppm. FTIR spectrum (KBr pellet): $\tilde{\nu} = 464$(W), 482(W), 526(VS), 552(M), 564(M), 574(M), 580(M), 608(W), 696(M), 706(S), 728(S), 740(M), 756(W), 772(W), 782(W), 808(W), 852(W), 988(W), 1018(W), 1042(W), 1066(W), 1080(W), 1096(W), 1154(M), 1180(S), 1220(W), 1252(W), 1288(W), 1298(M), 1350(W), 1374(M), 1386(W), 1420(W), 1428(M), 1440(M), 1652(W), 1732(VS), 2918(M), 2974 cm^{-1}(M). UV/Vis: 335, 405, 433, 502 nm. MALDI-TOF MS $m/z = 916$ amu [M^+].

Compound **IV** (46%): ^{1}H NMR (CS_2-acetone D6, 600 MHz): $\delta = 1.01$ (t, 3H), 1.7 (m, 2H), 2.86 (t, 2H), 3.21 (t, 2H), 4.01 (t, 2H), 7.15 (t, 1H), 7.51 ppm (m, 2H). ^{13}C NMR (CS_2-acetone D6, 150 MHz): $\delta =$ 11.04, 22.78, 30.32, 31.8, 45.13, 66.15, 79.78, 126.42, 126.85, 132.36, 138.41, 138.55, 140.82, 141.1, 142.16, 142.23, 142.26, 143.03, 143.04, 143.1, 143.15, 143.87, 143.89, 144.35, 144.63, 144.65,

144.74, 144.76, 144.87, 145.17, 145.25, 145.29, 145.32, 145.74, 147.3, 148.14, 170.82 ppm. FTIR spectrum (KBr pellet): $\tilde{\nu}$ = 480(W), 526(VS), 574(W), 578(W), 698(M), 742(W), 756(W), 782(W), 852(W), 1064(W), 1186(M), 1256(W), 1286(W), 1376(W), 1390(W), 1428(M), 1464(W), 1732(S), 2872(W), 2890(W), 2918(M), 2960 cm^{-1}(M). UV/Vis: 335, 405, 433, 502 nm. MALDI-TOF MS m/z = 930 amu [M^+].

Compound **V** (50%): ^{1}H NMR (CS_2-acetone D6, 600 MHz): δ = 1.01 (t, 3H), 1.44 (m, 2H), 1.64 (m, 2H), 2.85 (t, 2H), 3.22 (t, 2H), 4.05 (t, 2H), 7.15 (t, 1H), 7.50 ppm (m, 2H). ^{13}C NMR (CS_2-acetone D6, 150 MHz): δ = 14.39, 19.97, 30.34, 31.29, 31.83, 45.13, 64.43, 79.78, 126.41, 126.83, 132.33, 138.41, 138.57, 140.83, 141.1, 142.16, 142.23, 142.26, 143.03, 143.04, 143.11, 143.15, 143.87, 143.89, 144.36, 144.63, 144.65, 144.74, 144.76, 144.87, 145.17, 145.25, 145.29, 145.32, 145.73, 147.29, 148.13, 170.79 ppm. FTIR spectrum (KBr pellet): $\tilde{\nu}$ = 526(VS), 550(W), 574(M), 606(W), 696(S), 740(M), 808(W), 1174(S), 1184(M), 1220(W), 1250(M), 1288(M), 1368(W), 1392(W), 1412(M), 1428(M), 1444(M), 1464(M), 1734(S), 2866(M), 2890(M), 2922(M), 2952 cm^{-1}(M). UV/Vis: 335, 405, 433, 502 nm. MALDI-TOF MS m/z = 944 amu [M^+].

Compound **VI** (25%): ^{1}H NMR (CS_2-acetone D6, 600 MHz): δ = 1.02 (t, 3H), 1.69 (m, 2H), 2.75 (m, 6H), 4.03 (t, 2H), 7.10 (t, 1H), 7.43 (d, 1H), 7.47 ppm (d, 1H). ^{13}C NMR (CS_2-acetone D6, 150 MHz): δ = 11.13, 22.85, 30.86, 31.21, 31.55, 66.20, 70.55, 72.48, 126.14, 126.38, 126.45, 126.60, 126.67, 128.75, 129.80, 130.65, 130.79, 130.82, 130.87, 130.97, 131.86, 132.17, 132.77, 132.83, 133.78, 133.99, 137.51, 138.33, 139.42, 140.06, 140.49, 141.39, 141.67, 141.86, 142, 142.68, 142.82, 143.42, 143.48, 143.72, 143.84, 143.96, 144.02, 144.26, 144.32, 144.37, 144.47, 145.10, 145.82, 145.96, 146.02, 146.11, 146.36, 146.88, 147.03, 147.40, 147.50, 147.55, 147.83, 147.90, 148.33, 148.45, 148.53, 148.57, 148.61, 148.71, 149.17, 149.26, 149.39, 149.43, 150.52, 150.57, 150.77, 150.85, 151.12, 151.19, 151.45, 151.85, 152.12, 155.19, 155.70, 170.65 ppm. UV/Vis: 335, 405, 433, 502 nm. MALDI-TOF MS m/z = 900 amu [M^+].

Compound **VII** (30%): ^{1}H NMR (CS_2-acetone D6, 600 MHz): δ = 1.01 (t, 3H), 1.65 (m, 2H), 2.75 (m, 4H), 4.06 (t, 2H), 7.10 (t, 1H), 7.43 (d, 1H), 7.46 ppm (d, 1H). ^{13}C NMR (CS_2-acetone D6, 150 MHz): δ = 14.46, 20.04, 30.87, 31.23, 31.35, 64.48, 70.56, 72.48, 126.39, 126.45, 126.60, 128.75, 129.81, 130.66, 130.79, 130.82, 130.88, 130.98, 131.67, 131.85, 132.17, 132.78, 132.83, 133.78, 133.99, 137.51, 138.34, 139.43, 140.06, 140.50, 141.40, 141.67, 141.86, 142.01, 142.68, 142.83, 143.43, 143.48, 143.71, 143.85, 143.96, 144.02, 144.26, 144.32, 144.47, 145.10, 145.82, 145.96, 146.03, 146.11, 146.36, 146.88, 147.03, 147.41, 147.51, 147.54, 147.83, 147.9, 148.33, 148.46, 148.54, 148.61, 148.72, 149.17, 149.27, 149.39, 149.43, 150.53, 150.57, 150.77, 150.86, 151.12, 151.19, 151.46, 151.85, 152.12, 155.19, 155.71, 170.64 ppm. FTIR spectrum (KBr pellet): $\tilde{\nu}$ = 456(W), 532(M), 546(W), 558(W), 578(S), 642(M), 672(M), 698(S), 726(M), 738(M), 794(M), 828(M), 850(M), 1134(S), 1174(S), 1414(S), 1428(VS), 1728(VS), 2856(S), 2872(S), 2916(S), 2958 cm^{-1}(S). UV/Vis: 372, 406, 461, 536, 585, 619, 670 nm. MALDI TOF MS m/z = 1050 amu [M^+].

Compound **VIII** (33%): ^{1}H NMR (CS_2-acetone D6, 600 MHz): δ = 0.90 (t, 3H), 1.28 (m, 6H), 1.70 (m, 2H), 2.92 (t, 2H), 7.16 (t, 1H), 7.49 ppm(m, 2H). ^{13}C NMR (CS_2-acetone D6, 150 MHz): δ = 14.74, 23.48, 27.61, 30.3, 32.46, 34.96, 46.65, 80.3, 126.26, 126.38, 131.83, 138.27, 138.35, 139.54, 140.81, 141.09, 142.21, 142.25, 143.01, 143.02, 143.09, 143.14, 143.18, 143.88, 143.9, 144.3, 144.59, 144.62, 144.72, 144.8, 144.85, 144.87, 145.23, 145.26, 145.27, 145.3, 145.76, 147.86, 148.01, 148.43 ppm. FTIR spectrum (KBr pellet): $\tilde{\nu}$ = 458(M), 534(M), 558(W), 578(S), 642(M), 672(M), 700(M), 738(M), 794(M), 830(W), 852(W), 1020(W), 1066(W), 1080(W), 1134(M), 1178(M), 1232(M), 1290(M), 1416(S), 1428(VS), 1442(M), 1452(M), 1730(S), 2864(M), 2922(M), 2950 cm^{-1}(M). UV-VIS: 372, 406, 461, 536, 585, 619, 670 nm. MALDI-TOF MS m/z = 1064 amu [M^+].

Compound **IX** (30%): ^{1}H NMR (CS_2-acetone D6, 600 MHz): δ = 2.82 (m, 2H), 3.15 (m, 4H), 4.30 (s, 3H), 7.74 (t, 1H), 8.06 (d, 1H), 8.11 ppm(d, 1H). ^{13}C NMR (CS_2-acetone D6, 150 MHz): δ = 30.93, 34.06, 35.37, 51.05, 51.8, 71.18, 73.12, 126.14, 126.85, 126.89, 129.01, 129.73, 131.29, 131.43, 131.46, 131.51, 131.62, 132.08, 133.46, 133.48, 134.45, 134.66, 138.25, 139.02, 140.68, 140.69, 141.1, 142.06, 142.3, 142.49, 142.63, 143.31, 143.46, 144.06, 144.13, 144.35, 144.5, 144.6, 144.67, 144.97, 145.07, 145.09, 145.83, 146.47, 146.61, 146.69, 146.77, 147.01, 147.52, 147.69, 148.06, 148.13, 148.17, 148.2, 148.51, 148.53, 148.95, 149.1, 149.2, 149.24, 149.28, 149.35, 149.82, 149.86, 149.93, 150.06, 150.09, 151.17, 151.23, 151.43, 151.53, 151.76, 151.85, 152.12, 152.53, 152.8, 155.85, 156.38, 171.85, 172.18 ppm. FTIR spectrum (KBr pellet): $\tilde{\nu}$ = 458(W), 534(M), 578(M), 642(W), 672(M), 698(M), 726(W), 794(M), 830(VW), 850(W), 1134(M), 1156(W), 1170(M), 1194(W), 1230(W), 1246(W), 1416(S), 1428(VS), 1452(M), 1492(VW), 1566(W), 1636(W), 1736(S), 2910(M), 2924(M), 2940 cm^{-1}(M). UV/Vis: 372, 406, 461, 536, 585, 619, 670 nm. MALDI TOF MS m/z = 1036 amu [M^+].

Solubility determination

Solubilities of the investigated fullerene derivatives in organic solvents were determined using a procedure described earlier.[27]

X-ray structure determination for IV·C_6H_5Cl

Single-crystal synchrotron X-ray data were collected at 100 K at the BL14.1 at the BESSY storage ring (PSF at the Free University of Berlin, Germany) using a MAR225 detector, λ = 0.9050 Å. Structure solution with SHELXS97 and anisotropic structure refinements with SHELXL97. Crystal data for $C_{71}H_{14}O_2S{\cdot}C_6H_5Cl$: monoclinic, $P2_1/c$, a = 10.1000(2), b = 15.1889(3), c = 27.4564(8) Å, β = 90.137(1)°, V = 4212.0(2) Å^3, Z = 4, wR_2 = 0.490 (for 6402 reflections and 732 parameters) and R_1 = 0.215 [for 5831 reflections with $I > 2\sigma(I)$]. CCDC 715952 contains the supplementary crystallographic data for this paper. These data can be obtained free of charge from The Cambridge Crystallographic Data Centre via www.ccdc.cam.ac.uk/data_request/cif.

Characterization of fullerene/P3HT blends

Films for the AFM, optical microscopy, and PL measurements were prepared in the exact same manner as the active layer preparation for solar cells (see below) using ITO slides covered with PEDOT:PSS or clean glass slides as substrates. The AFM measurements were performed on a Dimension 3100 from Veeco.

For the PL measurements the sample was mounted in a home-built coldfinger cryostat and kept at liquid nitrogen temperature. The vacuum during the measurements was ca. 10^{-6} mbar. The excitation source was a VerdiV2 Laser from Coherent operating at 532 nm and at an output power of 10 mW. The photoluminescence light was focused on the entrance slit of a monochromator. In front of the entrance slit a set of different cut off filters were mounted. On the exit slit of the monochromator the detector is mounted. As detector a Si diode for the wavelength range up to 1100 nm was used. The signal of the detector was amplified and detected by a lock in amplifier (Standford Model SR 830). The obtained spectra were divided by the response function of the detector.

Preparation and characterization of solar cells

A fullerene derivative and P3HT were dissolved together in chlorobenzene to achieve polymer concentrations as high as 12 mg mL^{-1}. The weight ratio between the fullerene derivative and P3HT was varied between 1:2 and 5:6. The resulting fullerene/polymer solution was filtered through a 0.45 μm PTFE syringe filter. ITO glass slides with a size of 15×15 or 25×25 mm^2 were cleaned by successive sonication in toluene, acetone, and isopropyl alcohol. On the clean ITO surface PEDOT:PSS (Baytron PH) solution was spin-coated at 3000 rpm. The PEDOT:PSS films were annealed at 175 °C for 15 min. Afterwards, fullerene/polymer blends were spin-coated at 400–1500 rpm. The solar cell output parameters were virtually the same for devices with active layers deposited inside or outside the nitrogen glove-box. The films of the fullerene-polymer blends were dried in vacuum (ca. 10^{-3} mbar) at ambient temperature for 1–2 h. Afterwards, 100–200 nm thick aluminum top electrodes were deposited in high vacuum ca. 10^{-6} mbar and the finalized devices were annealed at temperatures of 155–160 °C for 5 min. For each binary system the optimal conditions were found experimentally: fullerene-derivative:P3HT component ratio, spin-coating frequency, and annealing temperature and time. Generally, the most reproducible and reliable recipe was using a 2:3 fullerene:P3HT ratio, 800 rpm spinning frequency, and device annealing at 160 °C for 5 min. *I–V* characteristics of the devices were obtained in dark and under the simulated 100 mW cm^{-2} AM1.5 solar irradiation provided by a KHS Steuernagel solar simulator. The intensity of the illumination was checked every time before the measurements using a calibrated silicon diode with known spectral response. All data given in this paper were not corrected for the mismatch between the solar simulator illumination and the AM1.5 spectrum. The photocurrent spectra were measured with a SRS 830 lock-in amplifier using the monochromated light from a 75 W Xe lamp as excitation.

Acknowledgements

P.A.T. thanks Dr. R. Koeppe for his assistance with the IPCE measurements and for valuable discussions. Financial support was provided by the Russian Ministry of Science and Education (contracts 02.513.11.3382 and 02.513.12.3103), the Russian Foundation for Basic Research (07–04–01742-a, 06–03–39007), and the Russian President Foundation (MK-4305.2009.3).

Keywords: fullerenes · heterojunctions · organic functional materials · photovoltaics · stacking interactions

[1] H. Hoppe, N. S. Sariciftci, *J. Mater. Res.* **2004**, *19*, 1924.
[2] J. Peet, J. Y. Kim, N. E. Coates, W. L. Ma, D. Moses, A. J. Heeger, G. C. Bazan, *Nat. Mater.* **2007**, *6*, 497.
[3] J. Y. Kim, K. Lee, N. E. Coates, D. Moses, T.-Q. Nguyen, M. Dante, A. J. Heeger, *Science* **2007**, *317*, 222.
[4] K. M. Coakley, M. D. McGehee, *Chem. Mater.* **2004**, *16*, 4533.
[5] H. Hoppe, N. S. Sariciftci, *J. Mater. Chem.* **2006**, *16*, 45.
[6] H. Hoppe, N. S. Sariciftci, *Advances in Polymer Science*, Springer, Berlin, **2008**.
[7] B. C. Thompson, J. M. J. Frechet, *Angew. Chem.* **2008**, *120*, 62; *Angew. Chem. Int. Ed.* **2008**, *47*, 58.
[8] D. Mühlbacher, M. Scharber, M. Morana, Z. Zhu, D. Waller, R. Gaudiana, C. Brabec, *Adv. Mater.* **2006**, *18*, 2884.
[9] J. C. Hummelen, B. W. Knight, F. Lepeq, F. Wudl, J. Yao, C. L. Wilkins, *J. Org. Chem.* **1995**, *60*, 532.
[10] M. M. Wienk, J. M. Kroon, W. J. H. Verhees, J. Knol, J. C. Hummelen, P. A. van Hall, R. A. J. Janssen, *Angew. Chem.* **2003**, *115*, 3493; *Angew. Chem. Int. Ed.* **2003**, *42*, 3371.
[11] a) http://www.solennebv.com (accessed December 2009); b) http://www.adsdyes.com/fullerenes.html (accessed December 2009); c) http://www.sesres.com/FullerenesPrices.asp (accessed December 2009); d) http://www.mtr-ltd.com/ (accessed December 2009).
[12] J. L. Hua, J. F. Meng, F. Ding, F. Li, H. Tian, *J. Mater. Chem.* **2004**, *14*, 1849.
[13] M. A. Loi, P. Denk, H. Hoppe, H. Neugebauer, C. Winder, D. Meissner, C. Brabec, N. S. Sariciftci, A. Gouloumis, P. Vazquez, T. Torres, *J. Mater. Chem.* **2003**, *13*, 700.
[14] F. Meng, J. Hua, K. Chen, H. Tian, L. Zuppiroli, F. Nuesch, *J. Mater. Chem.* **2005**, *15*, 979.
[15] M. Drees, H. Hoppe, C. Winder, H. Neugebauer, N. S. Sariciftci, W. Schwinger, F. Schaffler, C. Topf, M. C. Scharber, Z. Zhu, R. Gaudiana, *J. Mater. Chem.* **2005**, *15*, 5158.
[16] C. M. Atienza, G. Fernandez, L. Sanchez, N. Martin, I. S. Dantas, M. M. Wienk, R. A. J. Janssen, G. M. A. Rahman, D. M. Guldi, *Chem. Commun.* **2006**, 514.
[17] X. Wang, E. Perzon, J. L. Delgado, P. De La Cruz, F. Zhang, F. Langa, M. Andersson, O. Inganas, *Appl. Phys. Lett.* **2004**, *85*, 5081.
[18] L. Zheng, Q. Zhou, X. Deng, W. Fei, N. Bin, Z.-X. Guo, G. Yu, Y. Cao, *Thin Solid Films* **2005**, *489*, 251.
[19] N. Camaioni, L. Garlaschelli, A. Geri, M. Maggini, G. Possamai, G. Ridolfi, *J. Mater. Chem.* **2002**, *12*, 2065.
[20] N. Martín, *Chem. Commun.* **2006**, 2093.
[21] I. Riedel, E. von Hauff, J. Parisi, N. Martin, F. Giacalone, V. Dyakonov, *Adv. Funct. Mater.* **2005**, *15*, 1979.
[22] C.-H. Yang, J.-Y. Chang, P.-H. Yeh, T.-F. Guo, *Carbon* **2007**, *45*, 2951.
[23] C. Yang, J. Y. Kim, S. Cho, J. K. Lee, A. J. Heeger, F. Wudl, *J. Am. Chem. Soc.* **2008**, *130*, 6444.
[24] M. Lenes, G.-J. A. H. Wetzelaer, F. B. Kooistra, S. C. Veenstra, J. C. Hummelen, P. W. M. Blom, *Adv. Mater.* **2008**, *20*, 2116.
[25] S. A. Backer, K. Sivula, D. F. Kavulak, J. M. J. Frechet, *Chem. Mater.* **2007**, *19*, 2927.
[26] L. M. Popescu, P. van't Hof, A. B. Sieval, H. T. Jonkman, J. C. Hummelen, *Appl. Phys. Lett.* **2006**, *89*, 213507.
[27] P. A. Troshin, H. Hoppe, J. Renz, M. Egginger, J. Yu. Mayorova, A. E. Goryachev, A. S. Peregudov, R. N. Lyubovskaya, G. Gobsch, N. S. Sariciftci, V. F. Razumov, *Adv. Funct. Mater.* **2009**, *19*, 779.
[28] H. Pang, F. Vilela, P. J. Skabara, J. J. W. McDouall, D. J. Crouch, T. D. Anthopoulos, D. D. C. Bradley, D. M. de Leeuw, P. N. Horton, M. B. Hursthouse, *Adv. Mater.* **2007**, *19*, 4438.
[29] W. Ma, C. Yang, X. Gong, K. Lee, A. J. Heeger, *Adv. Funct. Mater.* **2005**, *15*, 1617.
[30] H. Hoppe, T. Glatzel, M. Niggemann, A. Hinsch, M. Ch. Lux-Steiner, N. S. Sariciftci, *Nano Lett.* **2005**, *5*, 269.
[31] P. W. M. Blom, V. D. Mihailetchi, J. A. Koster, D. E. Markov, *Adv. Mater.* **2007**, *19*, 1551.
[32] T. Erb, U. Zhokhavets, G. Gobsch, S. Raleva, B. Stuhn, P. Schilinsky, C. Waldauf, C. J. Brabec, *Adv. Funct. Mater.* **2005**, *15*, 1193.
[33] H. Hoppe, M. Niggemann, C. Winder, J. Kraut, R. Hiesgen, A. Hinsch, D. Meissner, N. S. Sariciftci, *Adv. Funct. Mater.* **2004**, *14*, 1005.
[34] C. J. Brabec, G. Zerza, G. Cerullo, S. D. Silvestri, S. Luzzatti, J. C. Hummelen, N. S. Sariciftci, *Chem. Phys. Lett.* **2001**, *340*, 232.
[35] S. E. Shaheen, C. J. Brabec, N. S. Sariciftci, F. Padinger, T. Fromherz, J. C. Hummelen, *Appl. Phys. Lett.* **2001**, *78*, 841.
[36] *Organic Syntheses. An Annual Publication of Satisfactory Methods for the Preparation of Organic Chemicals*, John Wiley & Sons, Vol. 25, **1945**, p. 19.
[37] *Organic Syntheses. An Annual Publication of Satisfactory Methods for the Preparation of Organic Chemicals*, John Wiley & Sons, Vol. 18, **1938**, p. 1.
[38] *Organic Syntheses. An Annual Publication of Satisfactory Methods for the Preparation of Organic Chemicals*, John Wiley & Sons, Vol. 26, **1946**, p. 1.
[39] J. V. Heid, R. Levine, *J. Org. Chem.* **1948**, *13*, 409.

Received: August 22, 2009
Revised: October 13, 2009
Published online on January 13, 2010

